A class of iron chelators with a wide spectrum of potent antitumor activity that overcomes resistance to chemotherapeutics

Megan Whitnall*, Jonathan Howard*, Prem Ponka†‡, and Des R. Richardson*‡

*Children's Cancer Institute Australia for Medical Research, Sydney, New South Wales 2031, Australia; and †Lady Davis Institute for Medical Research, McGill University, 3755 Cote-Ste-Catherine Road, Montreal, QC, Canada H3T 1E2

Novel chemotherapeutics with marked and selective antitumor activity are essential to develop, particularly those that can overcome resistance to established therapies. Iron (Fe) is critical for cell-cycle progression and DNA synthesis and potentially represents a novel molecular target for the design of new anticancer agents. The aim of this study was to evaluate the antitumor activity and Fe chelation efficacy of a new class of Fe chelators using human tumors. In this investigation, the ligands showed broad antitumor activity and could overcome resistance to established antitumor agents. The *in vivo* efficacy of the most effective chelator identified, di-2-pyridylketone-4,4,-dimethyl-3-thiosemicarbazone (Dp44mT), was assessed by using a panel of human xenografts in nude mice. After 7 weeks, net growth of a melanoma xenograft in Dp44mT-treated mice was only 8% of that in mice treated with vehicle. In addition, no differences in these latter animals were found in hematological indices between Dp44mT-treated mice and controls. No marked systemic Fe depletion was observed comparing Dp44mT- and vehicle-treated mice, probably because of the very low doses required to induce anticancer activity. Dp44mT caused up-regulation of the Fe-responsive tumor growth and metastasis suppressor *Ndrg1* in the tumor but not in the liver, indicating a potential mechanism of selective anticancer activity. These results indicate that the novel Fe chelators have potent and broad antitumor activity and can overcome resistance to established chemotherapeutics because of their unique mechanism of action.

cancer | di-2-pyridylketone-4,4-dimethyl-3-thiosemicarbazone | *Ndrg1*

Depriving cancer cells of the essential nutrient iron (Fe) is a novel approach for cancer treatment (1–3). Fe-containing proteins perform key reactions involved in energy metabolism and DNA synthesis. Indeed, the rate-limiting step of DNA synthesis is catalyzed by the Fe-containing enzyme ribonucleotide reductase (4). Moreover, chelators such as desferrioxamine (DFO) (Fig. 1*A*) arrest cells at the G_1/S interface, inhibiting cell-cycle progression and inducing apoptosis (5, 6).

Many *in vitro* and *in vivo* studies have shown that, compared with normal cells, cancer cells are more sensitive to Fe deprivation because of their marked Fe requirements (1–3). To facilitate rapid replication, neoplastic cells have significantly higher levels of ribonucleotide reductase and the transferrin receptor 1 (TfR1) (2, 3). The higher Fe utilization by cancer cells than their normal counterparts provides a rationale for the selective antitumor activity of chelators (1–3).

To date, the only chelator in widespread use for the treatment of Fe overload disease is DFO. In addition, DFO also has some antitumor activity (1–3). Recently, the Fe chelator Triapine (3-aminopyridine-2-carboxaldehyde thiosemicarbazone) (Fig. 1*A*), which inhibits ribonucleotide reductase activity and tumor growth *in vitro* and *in vivo* (7), has entered phase I and II clinical trials (2, 3). Additionally, some chelators of the pyridoxal isonicotinoyl hydrazone class (8) possess potent antitumor ac-
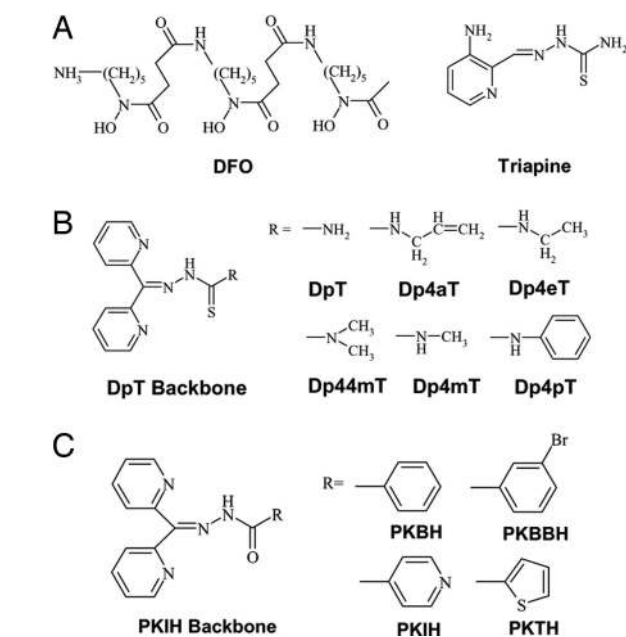

Fig. 1. Structures of agents. (*A*) DFO and Triapine. (*B*) DpT. (*C*) PKIH analogs.

tivity, e.g., 2-hydroxy-1-naphthylaldehyde isonicotinoyl hydrazone (9).

Studies of the structure–activity relationships of the pyridoxal isonicotinoyl hydrazone analogs led to the development of novel series of chelators showing significantly greater activity, the most effective being the di-2-pyridylketone thiosemicarbazone (DpT) and di-2-pyridylketone isonicotinoyl hydrazone (PKIH) analogs (Fig. 1 *B* and *C*) (10, 11). From preliminary screening, one of the most efficient of these chelators identified was di-2-pyridylketone-4,4,-dimethyl-3-thiosemicarbazone (Dp44mT) (Fig. 1*B*). This ligand showed selective antitumor activity and inhibited murine M109 lung carcinoma growth *in vivo* by 47% in 5 days (10). The cytotoxic mechanism of action of this chelator involved not only Fe chelation but also redox cycling of its Fe

complex to generate reactive oxygen species (ROS) (10). Moreover, in cultured cells Dp44mT resulted in marked up-regulation of the Fe-responsive tumor growth and metastasis suppressor *Ndrg1* (*N-myc downstream regulated gene-1*) (12). Up-regulation of *Ndrg1* suppresses primary tumor growth and metastasis (13, 14) and may be another mechanism by which chelators inhibit cancer cell proliferation.

Herein we investigated *in vitro* and, in particular, *in vivo* antitumor activity of our most effective PKIH and DpT chelators against human tumors. We show that these chelators have broad-spectrum activity against a wide range of cancer cell types *in vitro* and *in vivo*, including those possessing multidrug-resistant phenotypes.

Results

PKIH and DpT Fe Chelators Show High Antiproliferative Activity Against a Range of Tumor Cell Lines. Previously, the high antiproliferative activity of chelators of the PKIH and DpT classes of ligands were shown in a limited number of cell lines (10, 11). Here we examined 28 cell types to determine the spectrum of antitumor activity of the most effective PKIH and DpT analogs (Table 1, which is published as supporting information on the PNAS web site). DFO, 2-hydroxy-1-naphthylaldehyde isonicotinoyl hydrazone, Triapine, and the cytotoxic agent doxorubicin (DOX) were included as positive controls.

Of the 12 chelators tested, the least effective was DFO, with an IC_{50} value that ranged from 3 to >25 μM (Table 1). Dp44mT showed the greatest antitumor efficacy with an IC_{50} that ranged from 0.005 to 0.4 μM. The average IC_{50} of Dp44mT over 28 cell types was 0.03 ± 0.01 μM, which was significantly lower than that of Triapine (average IC_{50}: 1.41 ± 0.37 μM). Moreover, the antiproliferative activity of Dp44mT was greater than DOX in 26 of 28 cell lines. In fact, the average IC_{50} of DOX in the 28 cell types was 0.62 ± 0.35 μM. Related compounds to Dp44mT, namely PKBBH (di-2-pyridylketone 3-bromobenzoyl hydrazone), PKIH, PKTH (di-2-pyridylketone thiophenecarboxyl hydrazone), Dp4aT (di-2-pyridylketone 4-allyl-3-thiosemicarbazone), Dp4eT (di-2-pyridylketone 4-ethyl-3-thiosemicarbazone), Dp4mT (di-2-pyridylketone 4-methyl-3-thiosemicarbazone), and Dp4pT (di-2-pyridylketone 4-phenyl-3-thiosemicarbazone) (average IC_{50} over 25–28 cell lines = 0.57, 1.03, 0.88, 0.61, 0.77, 1.70, and 0.20 μM, respectively), also demonstrated appreciable activity that was not significantly different from DOX. The antiproliferative activity of Dp44mT was significantly more effective than all of the latter compounds.

Clonogenic Assays with Dp44mT. Clonogenic assays were used to assess the antitumor efficacy of Dp44mT. Fig. 2*A* shows the response of A2780 cells to a 48-h exposure to DFO, DOX, or Dp44mT. Even at the highest concentration of DFO (20 μM) or DOX (0.02 μM), colonies survived. In contrast, at its lowest concentration, Dp44mT (0.00125 μM) inhibited survival of A2780 clones by $\approx$50% compared with the control. At 0.0025 μM, Dp44mT completely prevented colony formation (Fig. 2*A*). Similar results were obtained for SK-N-MC cells (data not shown).

Dp44mT Retains Antiproliferative Activity in Drug-Resistant Cell Lines. Resistance of tumor cells to chemotherapeutics is a marked clinical problem (15). Hence, Dp44mT was assessed for its ability to overcome multidrug-resistant mechanisms in etoposide-resistant MCF-7/VP (16) clones of MCF-7 breast cancer cells and vinblastine-resistant KB-V1 (17, 18) clones of KB3-1 epidermoid carcinoma cells. To confirm resistance was maintained, etoposide (Fig. 2*B*) and vinblastine (Fig. 2*C*) were included as relevant controls. Etoposide-sensitive and -resistant cells were equally susceptible to the effects of Dp44mT, both resulting in an IC_{50} of 0.012 μM (Fig. 2*B*). These results indicated that
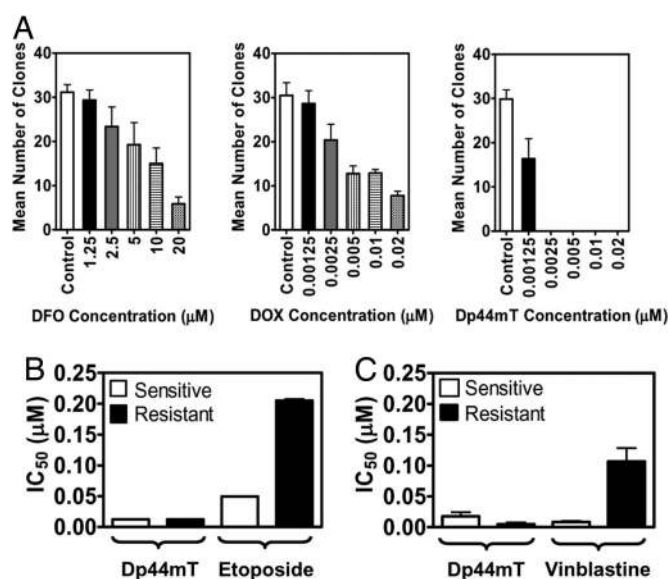
Fig. 2. Dp44mT markedly inhibits clonogenic formation and overcomes resistance to other cytotoxic agents. (*A*) Dp44mT is more effective than DFO and DOX at preventing clonogenic formation in A2780 human ovarian carcinoma. Cells were treated with chelators or DOX for 48 h, and outgrowth was assessed after 10–15 days in agent-free medium. (*B*) The MCF-7/VP cell line is resistant to etoposide compared with their sensitive parental counterpart, MCF-7. In contrast, the antiproliferative activity of Dp44mT was equally potent in these cells. (*C*) KB-V1 cells are resistant to vinblastine compared with their parental counterpart, KB3-1, whereas the antiproliferative activity of Dp44mT is greater in the resistant clone than the sensitive cell. Results are mean ± SD from three experiments.

resistance to etoposide did not interfere with the efficacy of Dp44mT.

Interestingly, vinblastine-resistant KB-V1 cells were more susceptible to Dp44mT than the vinblastine-sensitive parental cell line KB3-1 (Fig. 2*C*). As expected, the KB-V1 cell type remained resistant to vinblastine compared with the sensitive parental cells (KB3-1) (Fig. 2*C*). These results show that Dp44mT can overcome resistance to vinblastine.

Sensitivity of Tumor Cells to DpT Chelators Is Independent of p53 Status. Because numerous tumors contain functionally defective p53, anticancer agents that induce apoptosis in a p53-independent manner must be developed (19–22). Hence, we examined whether the DpT chelators can act independent of p53 apoptotic pathways. For all chelators, there was no correlation between p53 status and $-\log IC_{50}$ (data not shown), indicating that chelators act via a p53-independent mechanism to inhibit proliferation.

Dp44mT Markedly Inhibits the Growth of Human Tumor Xenografts *in Vivo*. Short-term studies. Fig. 3 *A*–*C* shows the effects of Dp44mT on the growth of established xenografts in mice. Much higher doses of Triapine (a positive control) than Dp44mT were required to observe significant antitumor activity. After 14 days of treatment, the average net tumor size of DMS-53 xenografts in control mice was 267 mm^3, whereas in Dp44mT (0.75 mg/kg per day)-treated mice, it was significantly reduced to 15 mm^3 (Fig. 3*A*). Notably, Dp44mT at a 16-fold lower dose (0.75 mg/kg per day), showed significantly greater antitumor activity than Triapine (12 mg/kg per day). A similar response to Dp44mT was also observed in SK-N-MC and SK-Mel-28 xenografts (Fig. 3 *B* and *C*).

Long-term studies. Rapid growth of SK-N-MC and DMS-53 xenografts meant for ethical reasons they could not be used for
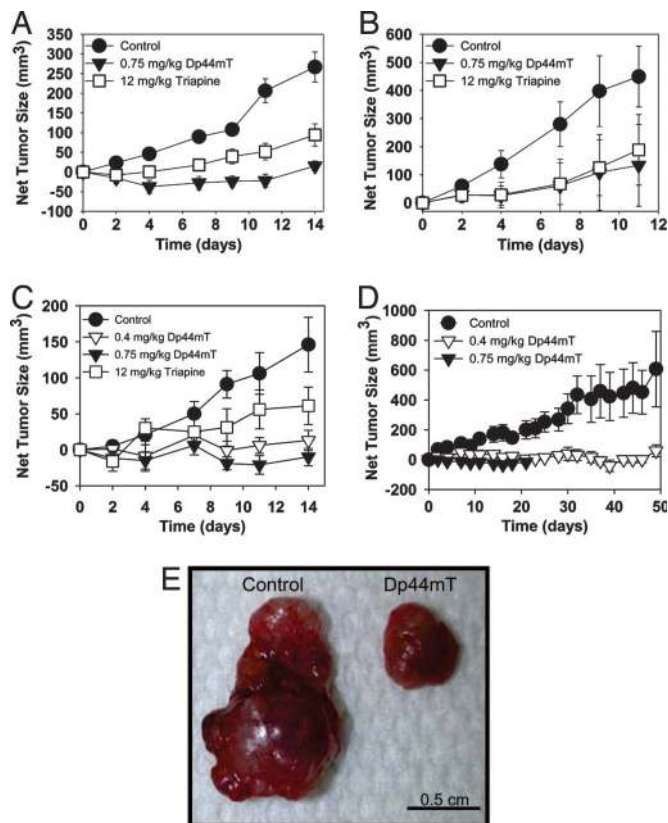
Fig. 3. Dp44mT is highly effective at inhibiting growth of a range of human xenografts in nude mice. Dp44mT (0.75 mg/kg per day) is equally or more effective than Triapine (12 mg/kg per day) at inhibiting growth of DMS-53 lung carcinoma (*A*), SK-N-MC neuroepithelioma (*B*), and SK-Mel-28 melanoma (*C*) tumor xenografts in nude mice when administered i.v. once per day, 5 days/week for up to 2 weeks. Each point represents mean ± SEM from 6–12 mice. (*D*) Dp44mT (0.4 or 0.75 mg/kg per day) inhibit SK-Mel-28 tumor xenografts in nude mice when given i.v. once per day, 5 days/week for up to 7 weeks. Each point represents mean ± SEM from six mice. (*E*) Photograph of SK-Mel-28 melanoma tumors taken from mice after 7 weeks with the vehicle or Dp44mT (0.4 mg/kg per day) using the regimen in *D*.

long-term studies, because the tumors in control mice became ulcerated after 2 weeks. In contrast, SK-Mel-28 xenografts grew at a slower rate, allowing extended treatment for 7 weeks (Fig. 3*D*).

Average net tumor size in Dp44mT (0.4 mg/kg per day)-treated mice (49 mm^3) was significantly smaller than in control mice (612 mm^3) after 7 weeks (Fig. 3 *D* and *E*). Tumor regression was also observed in mice treated with 0.75 mg/kg per day of Dp44mT. However, after 3 weeks of treatment at this latter dose, mice experienced a 14% decrease in body weight and, for ethical reasons, were killed. In contrast, at 0.4 mg/kg per day Dp44mT was well tolerated, with weight loss in mice not exceeding 10% over 7 weeks (see section below).

Biological Assessment After Chelator Treatment. Because Dp44mT is an Fe chelator (10), we assessed effects that Dp44mT may have on physiological processes. After 2 weeks, Dp44mT (0.75 mg/kg per day)-treated mice experienced significant weight loss compared with controls (Table 2, which is published as supporting information on the PNAS web site). However, no significant difference in weight loss was observed between mice receiving the lower dose of Dp44mT (0.4 mg/kg per day) and the controls after 7 weeks of treatment (Table 3, which is published as supporting information on the PNAS web site).

There was a significant ($P < 0.002$) increase in platelets and a slight but not significant ($P > 0.05$) increase in RBC counts in mice treated for 2 weeks with Dp44mT (0.75 mg/kg per day) compared with controls (Table 2). A significant ($P < 0.03$) decrease in RBC counts was observed in mice treated with Triapine (Table 2). Importantly, no significant ($P < 0.05$) differences in hematological indices were found using the lower Dp44mT dose (0.4 mg/kg per day) (Table 3) over 7 weeks.

After short-term treatment with Dp44mT (0.75 mg/kg per day) or vehicle control, no significant differences were detected in a range of serum biochemical parameters including creatine kinase in muscle and brain, aspartate aminotransferase, lactate dehydrogenase, alkaline phosphatase, alanine aminotransferase, total bilirubin, total protein, creatinine, and glucose (data not shown). However, mice treated with Triapine experienced a significant increase in alkaline phosphatase (185 ± 8; $n = 3$) compared with the control (115 ± 10; $n = 3$).

Organ Weights and Tissue Fe Levels After Dp44mT. No significant changes were found in organ-to-total-body-weight ratios in tumor-bearing mice comparing Dp44mT and control mice after short-term treatment (data not shown). In contrast, Triapine caused a significant increase (1.7-fold) in splenic weight when expressed as a percentage of total body weight (1.02 ± 0.06%; $n = 25$) compared with control mice (0.6 ± 0.03%; $n = 27$). In the long-term group, a significant increase in heart weight was observed after Dp44mT (0.4 mg/kg per day) (0.8 ± 0.06%; $n = 4$) compared with control mice (0.5 ± 0.01%; $n = 6$).

In short-term studies, there was a significant ($P < 0.004$) increase in liver Fe of Triapine-treated mice versus controls (Table 4, which is published as supporting information on the PNAS web site). There was also a significant ($P < 0.03$) decrease of brain Fe in Triapine-treated mice versus controls. A significant ($P < 0.03$) increase in splenic Fe was found in mice treated with Dp44mT (0.75 mg/kg per day) compared with the control (Table 4).

In long-term studies there was a significant decrease in liver Fe and a significant increase of heart Fe in Dp44mT-treated mice compared with controls (Table 5, which is published as supporting information on the PNAS web site). Interestingly, as found in short-term experiments (Table 4), there was a slight but not significant increase in tumor Fe comparing mice treated with Dp44mT and the control (Table 5).

Effects of Chelators on Tissue Histology and Blood Cell Morphology. After a 2-week treatment period with Triapine there were increased hematopoietic cells in the splenic red pulp compared with controls in hematoxylin and eosin-stained sections (asterisks) (compare Fig. 4 *Ai* and *Ci*). Perls staining of the spleen showed that, compared with the control (Fig. 4*Aii*), there was increased red pulp staining (consistent with hemosiderin) in Dp44mT- and Triapine-treated mice (asterisks) (Fig. 4 *Bii* and *Cii*). No splenic abnormalities were detected in mice bearing SK-Mel-28 xenografts after 7 weeks of therapy with Dp44mT (0.4 mg/kg per day) (data not shown).

In the 2-week studies myocardial lesions were found only in Dp44mT-treated mice (arrows in Fig. 4*Biii*). Such lesions consisted of poorly differentiated foci of necrosis, being replaced with immature fibrous tissue revealed by Gomori–Trichrome stain (arrows in Fig. 4*Biii*). Lesion severity was dose-dependent and was more marked at higher Dp44mT doses (0.75 mg/kg per day) than at lower doses (0.4 mg/kg per day). Because the lesions are fibrotic scar tissue, they are not reversible upon drug withdrawal. After 7 weeks of Dp44mT (0.4 mg/kg per day) treatment, some myocardial fibrosis was evident (data not shown), but it was not as pronounced as that at 0.75 mg/kg per day over 2 weeks.

Liver sections stained with hematoxylin and eosin from mice

MEDICAL SCIENCES
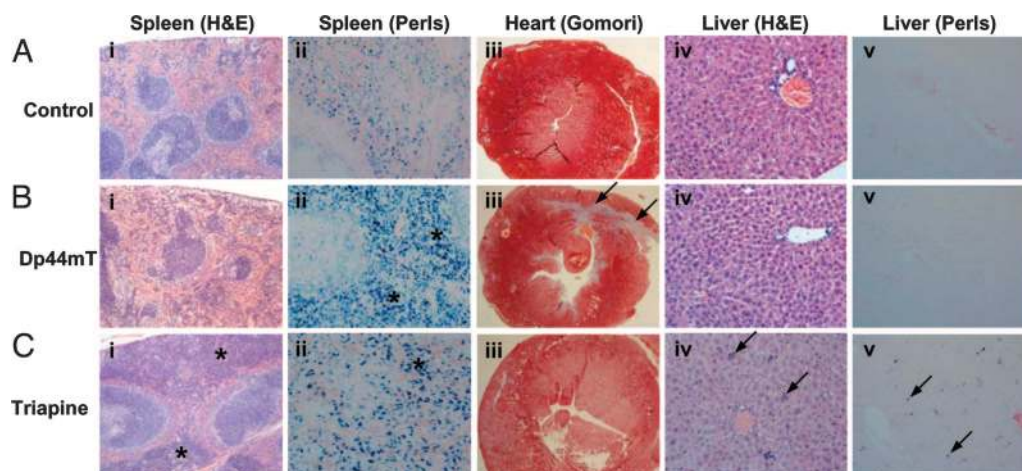
Fig. 4. Effect of Dp44mT and Triapine on spleen, heart, and liver histology. Histology from nude mice bearing DMS-53 lung carcinoma xenografts and treated i.v. with control (*A*), Dp44mT (0.75 mg/kg per day) (*B*), or Triapine (12 mg/kg per day) (*C*) once per day, 5 days/week for 2 weeks. (*i*) Hematoxylin and eosin-stained spleen. Asterisks denote increased hematopoiesis. (Magnification: ×40.) (*ii*) Perls-stained spleen. Asterisks denote increased Fe(III) deposits consistent with hemosiderin. (Magnification: ×200.) (*iii*) Gomori–Trichrome-stained cardiac tissue. Arrows denote fibrosis. (Magnification: ×20.) (*iv*) Hematoxylin and eosin-stained liver. Arrows denote hematopoietic cells. (Magnification: ×100.) (*v*) Perls-stained liver. Arrows denote Fe(III) deposits consistent with hemosiderin in Kupffer cells. (Magnification: ×100.)

treated over 2 weeks with Triapine demonstrated the presence of hematopoietic cells, present as either individual cells or small groups (arrows in Fig. 4*Civ*). Accompanying this change, there was a mild increase in Kupffer cell hemosiderin in the Triapine group as shown by Perls stain (arrows in Fig. 4*Cv*). No change in liver histology was observed after a 7-week treatment with Dp44mT (0.4 mg/kg per day; data not shown).

May–Grünwald/Giemsa-stained blood smears from mice demonstrated increased anisocytosis and polychromasia in only the Triapine-treated mice after 2 weeks (data not shown). Histological assessment of tumors from 2- and 7-week treatment groups indicated increased necrosis in chelator-treated mice compared with controls (data not shown). No alterations were observed in the brain or kidney over 2 or 7 weeks with any of the chelator doses (data not shown).

Expression of Fe-Regulated Genes in Liver and Tumor. Fe is crucial for proliferation, and studies *in vitro* have demonstrated that chelators up-regulate the expression of Fe-responsive genes such as the *TfR1*, which is involved in Fe uptake; *VEGF1*, which plays a role in angiogenesis; and the tumor growth and metastasis suppressor gene *Ndrg1* (12, 23). To understand the molecular events after Fe chelation, we performed RT-PCR examining the mRNA expression of *Ndrg1*, *TfR1*, and *VEGF1* in the liver (Fig. 5*A*) and tumor (Fig. 5*B*). This was done in mice bearing DMS-53 tumor xenografts after short-term treatment with vehicle only, Dp44mT (0.75 mg/kg per day), or Triapine (12 mg/kg per day).

A significant decrease in the expression of *Ndrg1*, *TfR1*, and *VEGF1* in the liver was noted for Dp44mT- and Triapine-treated animals (Fig. 5*A*). The decreased expression could be related to the increased liver Fe in both Dp44mT- and Triapine-treated mice (Table 4). In contrast, the expression of *Ndrg1*, *TfR1*, and *VEGF1* mRNA was significantly increased in the tumor (Fig. 5*B*). This observation was surprising because there was no decrease in tumor Fe observed in mice treated with chelators (Table 4). This finding could be explained by chelator-mediated changes in cellular Fe distribution that deprive the metal from certain compartments that control gene expression. Alternatively, *Ndrg1*, *VEGF1*, and *TfR1* are known to be regulated by the redox-sensitive transcription factor hypoxia-inducible factor 1 (HIF-1) (1, 12). HIF-1 is composed of a constitutively expressed β-subunit and an α-subunit regulated by hypoxia or Fe (1).

HIF-1α is regulated by prolyl hydroxylase; in the absence of Fe or oxygen, this enzyme is inactive, preventing binding by the von Hippel–Lindau protein and inhibiting its degradation by the proteasome (1). Previous studies showed that increased ROS can activate HIF-1α (24, 25). Because the Dp44mT–Fe complex is highly redox-active (10, 26), it can be speculated that ROS generation by this compound leads to increased transcription of these genes via HIF-1.

Discussion

The development of multidrug resistance (MDR) has become a significant obstruction in cancer treatment (16). Therefore, it is necessary to develop new chemotherapeutics. For many years, folate was targeted for antitumor drug development and resulted in the generation of highly successful therapeutics such as methotrexate, which prevents DNA synthesis. In contrast, strategies to target Fe for antitumor therapy have not been systematically explored. The present investigation is the first to conclusively demonstrate the marked antitumor efficacy of the novel Fe-chelating agent Dp44mT against a range of human tumors *in vivo*.

***In Vitro* Evaluation.** In this study we show the antiproliferative activity of the nine most effective PKIH and DpT chelators against 28 tumor lines (Table 1). Our results *in vitro* demonstrate their broad spectrum of activity and marked antiproliferative efficacy, with Dp44mT being particularly effective. Comparing average IC$_{50}$ values over the 28 cell lines, we observed that Dp44mT was 21 times more effective than DOX and 47 times more efficient than Triapine (Table 1).

The antitumor efficacy of Dp44mT and the related DpT chelators has previously been shown to be due to their ability to bind cellular Fe (10). In fact, synthesis of a DpT analog (known as Dp2mT), where the Fe-binding site is completely inactivated by methylation, prevented the ability of the compound to bind Fe and induce antitumor activity (10).

The marked activity of the DpT ligands is, in part, attributable to their lipophilicity, allowing them to permeate membranes and bind Fe pools more readily than less lipid-soluble chelators, e.g., DFO (9). Furthermore, upon PKIH and DpT ligands forming Fe complexes, these ligands generate cytotoxic ROS (10, 26–28). The resulting oxidative damage potentiates the antiproliferative
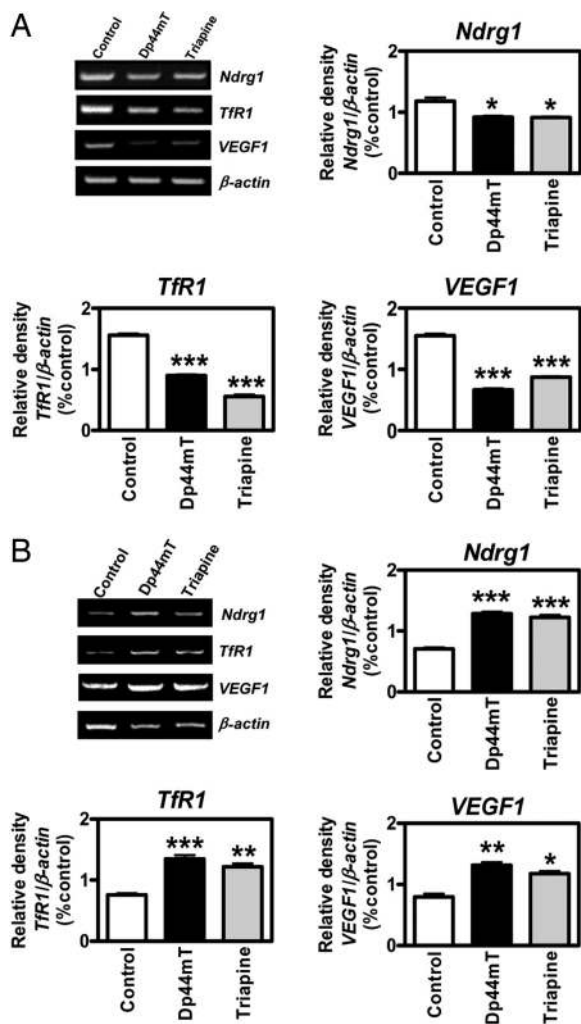
Fig. 5. Administration of Dp44mT and Triapine to mice up-regulates the growth and metastasis suppressor *Ndrg-1* in tumor xenografts but not the liver. Expression of the Fe-regulated genes *Ndrg1*, *TfR1*, and *VEGF1* is down-regulated in liver (*A*) and up-regulated in tumor (*B*) after treatment of nude mice bearing DMS-53 xenografts with Dp44mT (0.75 mg/kg per day) or Triapine (12 mg/kg per day) once per day, 5 days/week for 2 weeks. The densitometric results are mean ± SD from three experiments. *, $P < 0.05$; **, $P < 0.01$; ***, $P < 0.001$.

activity of PKIH and DpT chelators compared with 2-hydroxy-1-naphthylaldehyde isonicotinoyl hydrazone or DFO, which bind Fe but do not redox cycle (29). The higher activity of DpT series relative to the PKIH class can be ascribed, at least in part, to the electrochemical potentials of their Fe complexes (26, 28). In fact, the $Fe^{III/II}$ redox potentials of the $Fe(DpT)_2$ complexes (+153–225 mV) are much lower than the PKIH analogs (approximately +500 mV) and lie in a range accessible to cellular oxidants and reductants (26, 28).

The emergence of drug-resistant tumors remains a key chemotherapeutic problem (15). Attempts to reverse MDR by using MDR modulators have not yet generated optimal results (15). Considering this fact, etoposide and vinblastine resistance in tumor cells did not suppress the antiproliferative activity of Dp44mT (Fig. 2 *B* and *C*). Hence, Dp44mT may not be a substrate of ABC transporters such as P-glycoprotein and MDR-associated protein 1, which confer resistance to vinblastine (17) and etoposide (30), respectively. Clearly, the ability to overcome tumor resistance to established chemotherapeutics is an important advantage of Dp44mT.

Because of the role of p53 in cellular arrest and apoptosis, it was vital to assess the impact of p53 on chelator antiproliferative activity. Indeed, p53 mutations often result in a less favorable response to chemotherapy (20–22). In this study, p53 status did not affect DpT analog activity, indicating a p53-independent mechanism of antiproliferative activity, supporting their potential.

***In Vivo* Evaluation.** This is the first study to examine the effect of Dp44mT on human tumor xenografts and to show its broad spectrum of activity *in vivo*. We demonstrate that the antitumor activity of Dp44mT was far greater than Triapine. For instance, in 2-week studies Dp44mT (0.75 mg/kg per day) at a 16-fold-lower dose inhibited the growth of DMS-53 xenografts more profoundly than Triapine (12 mg/kg per day) (Fig. 3*A*). The striking antitumor activity of Dp44mT (0.75 mg/kg per day) in short-term experiments using melanoma cells (Fig. 3*C*) was sustained when treatment was extended to 7 weeks using 0.4 mg/kg per day (Fig. 3*D*). Moreover, at the lower Dp44mT dose cardiotoxicity was less marked.

It is significant that *in vivo* Dp44mT did not lead to marked Fe depletion of the tumor. Considering this finding, we suggest that it is the effect of the chelator entering the cancer cell, binding Fe, and forming the cytotoxic Fe complex (10, 26) that leads to its antitumor activity. In fact, we have shown that the antitumor efficacy of the DpT chelators is proportional to their effective redox activity (26).

The antitumor activity of Dp44mT in short-term and long-term studies was accompanied by little alteration in hematological and biochemical indices. The lack of a pronounced effect on hematological parameters e.g., RBC numbers, could be explained by the low chelator doses (0.4–0.75 mg/kg per day) required to induce antitumor activity. A marked increase in splenic Fe after Dp44mT treatment (Table 4) that was confirmed by Perls staining (Fig. 4*Bii*) may be related to increased RBC turnover. However, there was no change in hematological indices or splenic weight in these mice. Importantly, lower Dp44mT doses (0.4 mg/kg per day) over 7 weeks, which showed marked antitumor activity, had little effect on hematological indices (Table 3) or splenic Fe levels (Table 5).

In contrast to the observations with Dp44mT, more marked alterations in hematology were observed with Triapine (12 mg/kg per day). Evidence from histology, blood smears, and hematological indices of Triapine-treated mice (Fig. 4 and Table 2) indicated hematological toxicity, because of the high doses required to achieve antitumor activity. The pronounced increase in splenic erythropoiesis probably accounts for the rise in splenic weight in Triapine-treated mice. Our findings of hematological toxicity, together with evidence of anemia and met-hemoglobinemia in patients treated with Triapine (3), draw caution to claims that Triapine is a cytoprotectant (31).

One observation that requires note is the cardiac fibrosis observed in mice treated with the higher Dp44mT dose (0.75 mg/kg per day) (Fig. 4*Biii*). This effect may be due to the marked redox activity of the Dp44mT–Fe complex (10, 26). We suggest this because cardiotoxicity is observed with anthracyclines, which may induce this effect by ROS generation (32). Such damage may be avoided by coadministering Dp44mT with chelators, such as ICRF-187 (33) or DFO (34), or appropriate ROS scavengers. Here we show that the cardiotoxicity of Dp44mT was dose-dependent. Hence, optimization of the dose, route, and use of agents such as dexrazoxane will be required to prevent this side effect.

The ability of chelators to up-regulate the tumor growth and metastasis suppressor *Ndrg1* (12–14) could be vital for their anticancer efficacy. Our results showed that Dp44mT down-regulated these genes in mouse liver (Fig. 5*A*) but caused up-regulation in tumor xenografts (Fig. 5*B*). Hence, up-regulation of *Ndrg1* in tumors by Dp44mT may be important for understanding its selective anticancer activity.

It has been suggested that up-regulation of *TfR1* and *VEGF1* by chelators may enhance tumor growth via increased Fe uptake and angiogenesis, respectively (35). However, their growth-promoting effects are probably overwhelmed by the chelator-mediated inhibition of ribonucleotide reductase (36) and the up-regulation of *Ndrg1* and other molecules, because chelators markedly inhibit tumor growth (7, 10). This principle has also been observed with the chelator desferriexochelin (37). This ligand increased expression of the proapoptotic protein Nip1 and also VEGF1 but inhibited proliferation (37). The effects of chelators at inhibiting tumor growth are probably mediated through their action on many unique targets (e.g., Nip1, etc.) (19, 37, 38) and cannot be explained only by increased *Ndrg1*.

In conclusion, this study demonstrates the *in vivo* efficacy of Dp44mT at inhibiting a range of human tumors. In 2-week studies the efficacy of Dp44mT (0.75 mg/kg per day) was similar to or greater than a 16-fold-greater dose of Triapine in a number of human tumor xenografts. At 0.4 mg/kg per day over 7 weeks Dp44mT markedly inhibited melanoma growth and was well tolerated. Dp44mT caused *Ndrg1* up-regulation in the tumor but not the liver, indicating a potential mechanism of selective anticancer activity.

Materials and Methods

Chelators. The chelators were synthesized as described (26). Triapine was a gift from Vion Pharmaceuticals (New Haven, CT).

Cell Culture. HUH-7 hepatoma and CFPAC-1 pancreatic cancer lines were from M. Pourgholami (St. George Hospital, Sydney, Australia). The A2780 ovarian carcinoma cell line was from S. Clark (Garvan Institute, Sydney, Australia). The following were from R. Lock (Children's Cancer Institute Australia): MCF-7 breast cancer cells and their etoposide-resistant subclone MCF-7/VP (maintained in 4 μM etoposide); KB3-1 epidermoid carcinoma cells and their multidrug-resistant subclone KB-V1 (maintained in 0.1 μM vinblastine); and ALL3, ALL7, and ALL19 leukemic cells. Kelly neuroblastoma cells were from the European Collection of Cell Cultures (Wiltshire, U.K.). All other lines were from the American Type Culture Collection (Manassas, VA).

Clonogenic and Proliferation Assays. Clonogenic assays were performed by using standard procedures (19), and proliferation was assessed by the MTT method (9) [MTT, 3-(4,5-dimethylthiazol-2-yl)-5-(3-carboxymethoxyphenyl)-2-(4-sulfophenyl)-2*H*-tetrazolium].

Tumor Xenografts in Nude Mice and Chelator Administration. Female BALB/c nu/nu mice were used at 8–10 weeks of age. Tumor cells in culture were harvested, and 10^7 cells were suspended in Matrigel (BD Biosciences, San Jose, CA) and injected s.c. into the right flanks of mice. After engraftment, tumor size was measured by Vernier calipers. Tumor volumes (in cubic millimeters) were calculated as described (39). When tumor volumes reached 120 mm³, i.v. treatment began (day 0) (Fig. 3 *A–D*). Chelators were dissolved in 15% propylene glycol in 0.9% saline and injected i.v. over 5 consecutive days per week for up to 7 weeks. Control mice were treated with vehicle alone.

Hematology, Biochemistry, and Histology. Blood was collected by cardiac puncture. Hematologic and biochemical indices and tissue Fe were assayed by standard methods (40). Tissues were fixed in formalin for histology.

RNA Isolation and RT-PCR. Total RNA was isolated by using TRIzol (Invitrogen, Melbourne, Australia), and RT-PCR was performed (40). RT-PCR was shown to be semiquantitative by an optimization protocol, which demonstrated that it was in the log phase of amplification. β-Actin was used as an RNA loading control.

Statistical Analysis. Data were compared by using Student's *t* test. Results were expressed as mean ± SEM unless otherwise indicated. Data were considered statistically significant when *P* was <0.05.

1. Le NT, Richardson DR (2002) *Biochim Biophys Acta* 1603:31–46.
2. Buss JL, Greene BT, Turner J, Torti FM, Torti SV (2004) *Curr Top Med Chem* 4:1623–1635.
3. Kalinowski DS, Richardson DR (2005) *Pharmacol Rev* 57:547–583.
4. Thelander L, Reichard P (1979) *Annu Rev Biochem* 48:133–158.
5. Richardson DR, Milnes K (1997) *Blood* 89:3025–3038.
6. Brodie C, Siriwardana G, Lucas J, Schleicher R, Terada N, Szepesi A, Gelfand E, Seligman P (1993) *Cancer Res* 53:3968–3975.
7. Finch RA, Liu M, Grill SP, Rose WC, Loomis R, Vasquez KM, Cheng Y, Sartorelli AC (2000) *Biochem Pharmacol* 59:983–991.
8. Ponka P, Borova J, Neuwirt J, Fuchs O (1979) *FEBS Lett* 97:317–321.
9. Richardson DR, Tran EH, Ponka P (1995) *Blood* 86:4295–4306.
10. Yuan J, Lovejoy DB, Richardson DR (2004) *Blood* 104:1450–1458.
11. Becker EM, Lovejoy DB, Greer JM, Watts R, Richardson DR (2003) *Br J Pharmacol* 138:819–830.
12. Le NT, Richardson DR (2004) *Blood* 104:2967–2975.
13. Bandyopadhyay S, Pai SK, Gross SC, Hirota S, Hosobe S, Miura K, Saito K, Commes T, Hayashi S, Watabe M, Watabe K (2003) *Cancer Res* 63:1731–1736.
14. Kurdistani SK, Arizti P, Reimer CL, Sugrue MM, Aaronson SA, Lee SW (1998) *Cancer Res* 58:4439–4444.
15. Aouali N, Eddabra L, Macadre J, Morjani H (2005) *Crit Rev Oncol Hematol* 56:61–70.
16. Schneider E, Horton JK, Yang CH, Nakagawa M, Cowan KH (1994) *Cancer Res* 54:152–158.
17. Akiyama S, Fojo A, Hanover JA, Pastan I, Gottesman MM (1985) *Somat Cell Mol Genet* 11:117–126.
18. Shen DW, Cardarelli C, Hwang J, Cornwell M, Richert N, Ishii S, Pastan I, Gottesman MM (1986) *J Biol Chem* 261:7762–7770.
19. Abeysinghe RD, Greene BT, Haynes R, Willingham MC, Turner J, Planalp RP, Brechbiel MW, Torti FM, Torti SV (2001) *Carcinogenesis* 22:1607–1614.
20. O'Connor PM, Jackman J, Bae I, Myers TG, Fan S, Mutoh M, Scudiero DA, Monks A, Sausville EA, Weinstein JN, *et al.* (1997) *Cancer Res* 57:4285–4300.
21. Lowe SW (1995) *Curr Opin Oncol* 7:547–553.
22. Guimaraes DP, Hainaut P (2002) *Biochimie* 84:83–93.
23. Richardson DR (2005) *Curr Med Chem* 12:2711–2729.
24. Park JH, Kim TY, Jong HS, Chun YS, Park JW, Lee CT, Jung HC, Kim NK, Bang YJ (2003) *Clin Cancer Res* 9:433–440.
25. Chandel NS, McClintock DS, Feliciano CE, Wood TM, Melendez JA, Rodriguez AM, Schumacker PT (2000) *J Biol Chem* 275:25130–8.
26. Richardson DR, Sharpe PC, Lovejoy DB, Senaratne D, Kalinowski DS, Islam M, Bernhardt PV (2006) *J Med Chem*, in press.
27. Chaston TB, Watts RN, Yuan J, Richardson DR (2004) *Clin Cancer Res* 10:7365–7374.
28. Bernhardt PV, Caldwell LM, Chaston TB, Chin P, Richardson DR (2003) *J Biol Inorg Chem* 8:866–880.
29. Richardson DR, Bernhardt PV (1999) *J Biol Inorg Chem* 4:266–273.
30. Yang CH, Huang CJ, Yang CS, Chu YC, Cheng AL, Whang-Peng J, Yang PC (2005) *Cancer Res* 65:6943–6949.
31. Jiang ZG, Lu XC, Nelson V, Yang X, Pan W, Chen RW, Lebowitz MS, Almassian B, Tortella FC, Brady RO, Ghanbari HA (2006) *Proc Natl Acad Sci USA* 103:1581–1586.
32. Xu X, Persson HL, Richardson DR (2005) *Mol Pharmacol* 68:261–271.
33. Hasinoff BB, Schnabl KL, Marusak RA, Patel D, Huebner E (2003) *Cardiovasc Toxicol* 3:89–99.
34. Saad SY, Najjar TA, Al-Rikabi AC (2001) *Pharmacol Res* 43:211–218.
35. Linden T, Wenger RH (2003) *Int J Cancer* 106:458–459.
36. Green DA, Antholine WE, Wong SJ, Richardson DR, Chitambar CR (2001) *Clin Cancer Res* 7:3574–3579.
37. Chong TW, Horwitz LD, Moore JW, Sowter HM, Harris AL (2002) *Cancer Res* 62:6924–6927.
38. Gao J, Richardson DR (2001) *Blood* 98:842–850.
39. Balsari A, Tortoreto M, Besusso D, Petrangolini G, Sfondrini L, Maggi R, Menard S, Pratesi G (2004) *Eur J Cancer* 40:1275–1281.
40. Dunn LL, Sekyere EO, Rahmanto YS, Richardson DR (May 16, 2006) *Carcinogenesis*, 10.1093/carcin/bgl045.